SHAPING THE GLOBULAR CLUSTER MASS FUNCTION BY STELLAR-DYNAMICAL EVAPORATION

DEAN E. MCLAUGHLIN
University of Leicester, Department of Physics and Astronomy, University Road, Leicester, UK LE1 7RH

AND

S. MICHAEL FALL
Space Telescope Science Institute, 3700 San Martin Drive, Baltimore, MD 21218
ApJ, submitted

ABSTRACT

Dynamical-evolution models of old globular cluster mass functions (GCMFs), in which the depletion of an initial power-law distribution at low masses is caused predominantly by evaporation driven by internal two-body relaxation, can explain the turnover mass scale $M_{\rm TO}$ and the generic shape of the GCMF at $M < M_{\rm TO}$. We point out that such models inherently predict that the GCMF should depend on the cluster half-mass density, ρ_h, and we show that the Galactic GCMF exhibits precisely the expected variations: $M_{\rm TO}$ increases systematically with ρ_h, while the width of the distribution decreases. The quantitative details are consistent with a cluster mass-loss rate, $-dM/dt = \mu_{\rm ev} \propto \rho_h^{1/2}$ with ρ_h approximately constant in time, which we adopt as the simplest description of evaporation. The normalization of $\mu_{\rm ev}$ is within a factor of two of standard theoretical expectations. We show that the known, weak dependence of the Milky Way GCMF on Galactocentric position $r_{\rm gc}$ results from its basic dependence on cluster density plus a very scattered $\rho_h(r_{\rm gc})$ distribution, which we take directly from observations. This effectively removes the weakness of radial GCMF variations as an argument against an evaporation-dominated, evolutionary origin for the peak and low-mass behavior of the distribution. Similarly, a previously noted difference between the mass functions of low- and high-concentration Galactic globulars follows directly from the dependence on ρ_h, combined with differences in the ρ_h distribution at low and high cluster concentrations; it does not require distinct mass-loss laws for GCs in these two regimes.

Subject headings: galaxies: star clusters—globular clusters: general

1. INTRODUCTION

The globular cluster mass function (GCMF, or $dN/d\log M$) is the number of old globular clusters (GCs) per unit logarithmic cluster mass in a galaxy. It is roughly proportional to the GC luminosity function, defined observationally as the number of GCs per unit magnitude. The distribution peaks, or turns over, at a mass scale $M_{\rm TO} \approx 1\text{–}2 \times 10^5 M_\odot$, which is very similar in most galaxies (Harris 2001; Jordán et al. 2006). The number of clusters declines rapidly towards higher masses, in a way strongly reminiscent of the power-law mass distributions, $dN/d\log M \propto M^{1-\beta}$ with $\beta \approx 2$, of molecular clouds and of massive young clusters in the Milky Way and nearby galaxies (Harris & Pudritz 1994; Elmegreen & Efremov 1997). This part of the GCMF therefore appears to be intimately connected to cluster formation processes.

Old GCMFs also fall towards lower masses $M < M_{\rm TO}$, eventually tending to $dN/d\log M \propto M^{+1}$, or $\beta \simeq 0$ (Fall & Zhang 2001; McLaughlin 1994; Jordán et al. 2007). By contrast, young cluster mass functions rise steeply towards these low masses, adhering to the same $\beta \simeq 2$ power law that holds for them at higher M (e.g., Zhang & Fall 1999). A natural hypothesis is that this difference is primarily age-related, resulting from the preferential destruction of low-mass GCs as they orbit for a Hubble time in their parent galaxies (Fall & Rees 1977).

The cluster mass-loss mechanisms relevant on Gyr timescales are stellar evolution, gravitational shocks during disk and bulge passages, and stellar escape driven by internal two-body relaxation (evaporation). But, unless special initial conditions are invoked (Vesperini & Zepf 2003), stellar evolu-

tion removes a constant mass *fraction* from every cluster and thus does not change the shape of the GCMF (Fall & Zhang 2001). Then, for realistic GC parameters in the Milky Way the integrated mass loss from gravitational shocks is generally much smaller than that from two-body relaxation (see Fall & Zhang 2001; Prieto & Gnedin 2006; Jordán et al. 2007). In addition, for a given cluster density shocks are more important at high masses than at low masses. Relaxation-driven evaporation is therefore the logical main focus of models in which a young cluster mass function rising towards low M is transformed by dynamical evolution into a peaked GCMF in old age.

Evaporation operates on multiples of the half-mass relaxation timescale, $t_{\rm rh} \propto (M r_h^3)^{1/2}/\ln \Lambda$, where r_h is the (three-dimensional) half-mass radius and $\ln \Lambda$ is the usual Coulomb logarithm (e.g., Section 8.3 of Binney & Tremaine 1987). Ignoring the slow variation of the logarithm, the instantaneous mass-loss rate of an evaporating cluster is given to first order by $-dM/dt = \mu_{\rm ev} \propto M/t_{\rm rh} \propto \rho_h^{1/2}$, where $\rho_h \equiv 3M/8\pi r_h^3$ is the half-mass density. Fall & Zhang (2001) argue that ρ_h is conserved in time for any single cluster, leading to a linear dependence of total mass on time: $M = M_0 - \mu_{\rm ev} t$. This $M(t)$ behavior, which is confirmed by numerical simulations of evaporation (Vesperini & Heggie 1997; Gnedin, Lee, & Ostriker 1999; Giersz 2001; Baumgardt & Makino 2003), implies a GCMF peak at $M_{\rm TO} \sim \mu_{\rm ev}\tau$ for a system of coeval clusters with given ρ_h and age τ: initially less massive GCs are disrupted completely, and replaced with the remnants of objects that began with $M_0 > \mu_{\rm ev}\tau$. Moreover, because all surviving clusters have lost the same *total* amount of mass, $dN/d\log M$ always scales as $\propto M^{+1}$ (or $\beta = 0$) in the limit $M \ll \mu_{\rm ev}\tau$, as observed; see Fall & Zhang (2001) or Jordán et al. (2007).

Gravitational shocks can then be thought of approximately as giving a larger effective $\mu_{\rm ev}$ without altering the fundamental linearity of M versus time (see Figure 1 of Fall & Zhang; also Gnedin, Lee, & Ostriker 1999).

Fall & Zhang (2001) successfully fit the mass function of the entire Milky Way GC system with semi-analytical models of evolution from an initial low-mass $dN/d\log M_0 \propto M_0^{1-\beta}$ with $\beta = 2$. They include details of cluster mass loss due to stellar evolution and gravitational shocks as well as evaporation by two-body relaxation at constant ρ_h, although as just outlined the last is most important. Jordán et al. (2007) fit GCMF data from 89 early-type members of the Virgo Cluster using a simple analytical function that contains a single parameter, $\widehat{\Delta} \equiv \widehat{\mu}_{\rm ev}\tau$, representing the total mass lost from every GC at a typical density $\widehat{\rho}_h$ in each system. They find a rather modest dependence of $\widehat{\Delta}$ on galaxy luminosity, which is essentially consistent with the expected $\widehat{\mu}_{\rm ev} \propto \widehat{\rho}_h^{1/2}$ for evaporation-dominated mass loss, given that variations of GC density with $L_{\rm gal}$ are themselves slight (Jordán et al. 2005). This then appears to be the main explanation for the observation that $M_{\rm TO} \sim \widehat{\mu}_{\rm ev}\tau$ varies only weakly as a function of $L_{\rm gal}$ in general; see Jordán et al. (2007) for more details.

Models along these lines for the GCMF are thus successful in global terms. But they also make one prediction that has yet to be tested directly against any data: in a system of GCs covering a wide range of ρ_h and thus $\mu_{\rm ev}$, the peak mass $M_{\rm TO}$ and the overall GCMF shape should depend on ρ_h. In this paper we show that this is in fact the case in the Milky Way, and that the observed GCMF variations are quantitatively well fit by the basic assumption of a time-independent $\mu_{\rm ev} \propto \rho_h^{1/2}$ for any cluster.

We also show that combining a relatively strong dependence of the GCMF on ρ_h with the observed distribution of ρ_h over Galactocentric position, $r_{\rm gc}$, leads—since any $\rho_h(r_{\rm gc})$ correlation is very scattered—to $dN/d\log M$ depending only weakly on $r_{\rm gc}$. This result is well known in the Milky Way and other large galaxies (Harris 2001; Barmby, Huchra, & Brodie 2001; Harris, Harris, & McLaughlin 1998; Jordán et al. 2007). It has been used to argue against the whole notion that $M_{\rm TO}$ and the low-mass GCMF developed primarily through the relaxation-driven evaporation of clusters (Vesperini et al. 2003). We stress here that such criticisms really only point to the inadequacies of past attempts to explain the complicated $\rho_h(r_{\rm gc})$ distributions in GC systems—a secondary problem that is distinct from the main idea and its predictions for $dN/d\log M$ as a function of cluster ρ_h.

2. THE GALACTIC GCMF AS A FUNCTION OF CLUSTER DENSITY

2.1. *Cluster Masses, Densities, and Galactocentric Radii*

As the first step towards constructing GCMFs for the Milky Way, Figure 1 shows the distribution of cluster mass M against the half-mass density ρ_h and against Galactocentric radius $r_{\rm gc}$, as well as the distribution of ρ_h versus $r_{\rm gc}$ that links the two mass plots. This is all for 146 GCs with absolute V magnitudes recorded in the catalogue of Harris (1996).[1] Masses follow from applying the individual population-synthesis model mass-to-light ratios Υ_V computed (for an assumed age of 13 Gyr) by McLaughlin & van der Marel (2005), after first multiplying every one by 0.8 to give a median $\widehat{\Upsilon}_V \simeq 1.5 M_\odot L_\odot^{-1}$ in

keeping with direct dynamical estimates (McLaughlin 2000; McLaughlin & van der Marel 2005; Barmby et al. 2007). Harris (1996) gives the projected half-light radius R_h for 141 of the clusters with a mass estimated in this way. For these we obtain the three-dimensional half-mass radius from the general rule $r_h = (4/3)R_h$ (Spitzer 1987), and then $\rho_h = 3M/8\pi r_h^3$. The remaining objects, with masses M_i ($i = 1, \ldots, 5$), have no R_h measurements; to each of these in turn we assign a ρ_h equal to the median value for those of the first 141 clusters having masses within a factor two of M_i.

The left-hand panel in Figure 1 shows a strong dependence of the cluster mass distribution on half-mass density: the median $\widehat{M}$ increases with ρ_h, while the dispersion in $\log M$ decreases. The first of these points is related to the well known fact that r_h correlates rather poorly with M (e.g., McLaughlin 2000). The second point, that the GCMF dispersion decreases with increasing ρ_h, appears not to have been noticed before. We return to this in §2.2 below.

The dashed line in the plot of M versus ρ_h traces the proportionality $M \propto \rho_h^{1/2}$, or equivalently $Mr_h^3 = $ constant. Insofar as the half-mass relaxation time scales approximately as $t_{\rm rh} \propto (Mr_h^3)^{1/2}$ and the mass-loss rate as $\mu_{\rm ev} \propto \rho_h^{1/2}$, if ρ_h is constant in time for each GC, then all those falling along a line parallel to the one shown have the same lifetime against evaporation. (Recall that $Mr_h^3 = $ constant also defines the lower leg of the GC "survival triangle" when the M–ρ_h plot is recast as r_h versus M; see Fall & Rees 1977 and Gnedin & Ostriker 1997). The fact that such a locus nicely bounds the lower envelope of the observed cluster distribution already hints strongly that evaporation through two-body relaxation has modified the GCMF at low masses. The question remaining is whether the observed $dN/d\log M$ is consistent with this interpretation in quantitative detail. We show in the next subsection that it is.

All previous studies of GCMF variations, in any galaxy, have passed over the issue of ρ_h dependence to focus instead on the mass distribution as a function of galactocentric position, which is shown for the Milky Way in the middle panel of Figure 1. This is, of course, essentially a convolution of M versus ρ_h in the left-hand panel with ρ_h versus $r_{\rm gc}$ in the rightmost plot. The much weaker dependence of cluster M on $r_{\rm gc}$, relative to that of M on ρ_h, is thus easily seen to be the result of an ambiguous and highly scattered $\rho_h(r_{\rm gc})$ distribution. It is in attempting to understand this complex situation in simple terms that most models of GCMF evolution have run into difficulty.

If the GCMF is fundamentally a function of cluster density because $\mu_{\rm ev} \propto \rho_h^{1/2}$, then predicting spatial variations of $dN/d\log M$ in a model requires first relating ρ_h to $r_{\rm gc}$. Nearly all authors to date (e.g., Murali & Weinberg 1997; Baumgardt 1998; Vesperini 1998; Fall & Zhang 2001) have done this by assuming that GC densities are set by tidal limitation at the pericenters r_p of their orbits in static, spherical, logarithmic galaxy potentials; thus, $\rho_h \propto r_p^{-2}$ and the GCMF peak at any age τ scales as $M_{\rm TO} \sim \mu_{\rm ev}\tau \propto r_p^{-1}$. Accounting for the observed near-invariance of $M_{\rm TO}$ with the current position $r_{\rm gc}$—or, equivalently, for the very large scatter about any line like $\rho_h \propto r_{\rm gc}^{-2}$ in Figure 1—then requires some dynamical mechanism to distribute clusters with a narrow range of r_p, ρ_h, and $M_{\rm TO}$ over a wide range of $r_{\rm gc}$.

Fall & Zhang (2001) show that a strong, $r_{\rm gc}$-dependent radial-orbit bias in the initial Milky Way cluster system could

---

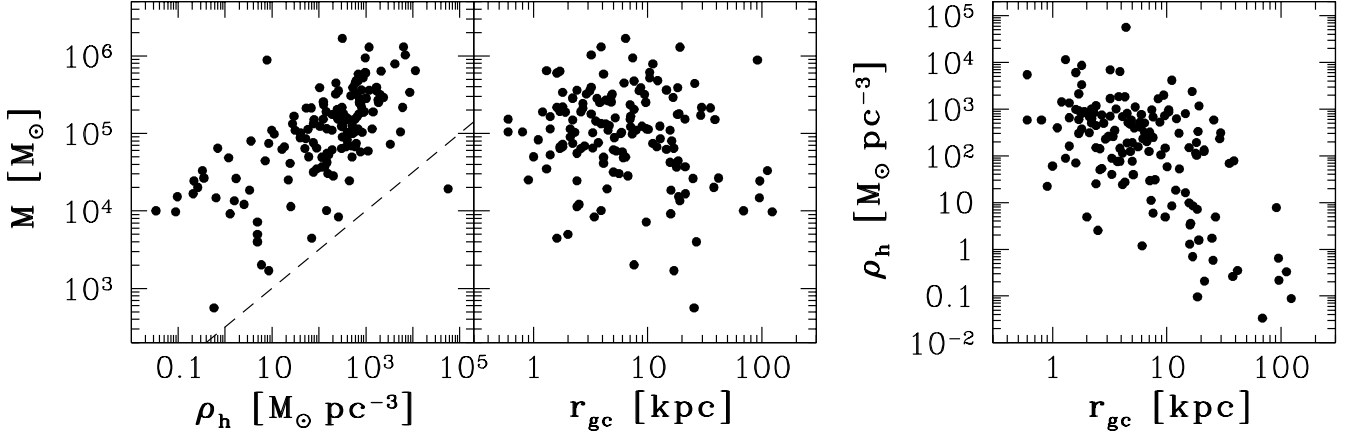[1] Feb. 2003 version; see http://physwww.mcmaster.ca/~harris/mwgc.dat .

FIG. 1.— *Left:* Mass versus three-dimensional half-mass density, $\rho_h \equiv 3M/8\pi r_h^3$, and versus Galactocentric radius, $r_{\rm gc}$, for 146 Milky Way GCs in the catalogue of Harris (1996). The dashed line in the first panel is $M \propto \rho_h^{1/2}$, a locus of constant lifetime against evaporation. *Right:* Half-mass density versus $r_{\rm gc}$ for the same clusters. The poor definition and large scatter of this correlation is responsible for the difficulties in all dynamical-evolution models to date that have attempted to explain the weakness or even absence of any $r_{\rm gc}$ dependence in the GCMF.

achieve the required spatial mixing if the Galaxy were spherical and static. But Vesperini et al. (2003) point out that such initial conditions are probably inconsistent with the observed isotropy of present-day GC velocity distributions, both in the Milky Way and especially in the Virgo elliptical M87 (where $M_{\rm TO}$ is also effectively constant as a function of $r_{\rm gc}$). They argue from this that the peak and low-mass shape of the GCMF are not the result of dynamical evolution after all. However, this reasoning omits the fundamental point that (in the Milky Way, at least) $dN/d \log M$ does depend on ρ_h; and it discounts altogether an evolutionary explanation for this fact, based only on the shortcomings of a secondary hypothesis invoked to explain the dependence of ρ_h on $r_{\rm gc}$ under restrictive, idealized assumptions about the Galactic potential.

In what follows, we compare the behavior of $dN/d \log M$ as a function of ρ_h in the Milky Way with simple models for the evolution of the GCMF when cluster disruption is driven predominantly by internal two-body relaxation; and we use the observed dependence of ρ_h on $r_{\rm gc}$ in Figure 1 exactly as given, to show that our models produce the required weak variation of the GCMF with Galactocentric radius. We do not attempt to explain the origin of the current $\rho_h(r_{\rm gc})$ distribution, nor do we ask how any cluster obtained its ρ_h initially. As Fall & Zhang (2001), Prieto & Gnedin (2006), and Jordán et al. (2007) all have discussed, a better understanding of these important questions will most likely come from abandoning the direct linkage of ρ_h to a fixed r_p in a monolithic galaxy potential, which has framed the debate so far. In future, simulations should instead be used to follow the evolution of GC systems in non-spherical, time-varying galaxies undergoing violent relaxation, major mergers, and multiple accretion events within a realistic hierarchical cosmology.

2.2. $dN/d \log M$ versus ρ_h and $r_{\rm gc}$

We assume that the mass-loss rate of any cluster is constant in time, and therefore that the total mass decreases linearly with time. This simple behavior is seen in numerical simulations of two-body relaxation, either acting alone or augmented by gravitational shocks (Vesperini & Heggie 1997; Gnedin, Lee, & Ostriker 1999; Giersz 2001; Baumgardt & Makino 2003). To achieve this given our approximation that $\mu_{\rm ev} \propto \rho_h^{1/2}$ for relaxation-driven evaporation clearly requires

that ρ_h be conserved to first order as both M and r_h decrease. The impression sometimes gained from the literature is that it is r_h, rather than ρ_h, which is more nearly constant in clusters evaporating by internal relaxation. However, careful inspection of results from a number of simulations (Aarseth & Heggie 1998; Gnedin, Lee, & Ostriker 1999; Giersz 2001) shows that r_h does decrease modestly, in a fashion generally consistent with $r_h(t) \sim M(t)^{1/3}$ and thus $\rho_h \simeq$ constant. This is particularly accurate after clusters have gone through core collapse.

To develop a model for the GCMF from this, consider first a group of coeval GCs with an initial mass function $dN/d \log M_0$ and a single, time-independent mass-loss rate $\mu_{\rm ev}$. The mass of every such cluster decreases as $M = M_0 - \mu_{\rm ev}t$, until at any fixed age τ each has lost the same total amount $\Delta \equiv M_0 - M = \mu_{\rm ev}\tau$. In this case, the evolved and initial GCMFs are related by (see Fall & Zhang 2001)

$$\frac{dN}{d \log M} = \frac{M}{M_0} \times \frac{dN}{d \log M_0} = \frac{M}{M+\Delta} \frac{dN}{d \log (M+\Delta)} . \quad (1)$$

As Fall & Zhang first noted, a linear dependence of cluster mass on time thus leads generically to $dN/d \log M \propto M^{+1}$ (in linear terms, $dN/dM \to$ constant) in the limit $M \ll \Delta$, irrespective of any details of the initial mass function.

We follow Fall & Zhang (2001) and Jordán et al. (2007) in adopting a Schechter (1976) function for the initial GCMF:

$$dN/d \log M_0 \propto M_0^{1-\beta} \exp\left(-M_0/M_c\right) . \quad (2)$$

With $\beta \simeq 2$, this distribution describes the power-law mass functions of young massive clusters in systems like the Antennae galaxies (e.g., Zhang & Fall 1999). An exponential cut-off scale $M_c \sim 10^6 M_\odot$ is consistent with these data, even if not always demanded by them; here we require it mainly to match the curvature observed at high masses in old GCMFs (see Jordán et al. 2007; Burkert & Smith 2000).

Combining equations (1) and (2) gives the probability density that a single GC with some known Δ has a mass M. The final GCMF of a system of $\mathcal{N}$ GCs with a range of mass-loss rates (or ages, or both) is then just the sum of all individual probability densities:

$$\frac{dN}{d \log M} = \sum_{i=1}^{\mathcal{N}} \frac{A_i M}{[M+\Delta_i]^\beta} \exp\left[-\frac{M+\Delta_i}{M_c}\right] , \quad (3)$$

TABLE 1
MILKY WAY GC PROPERTIES IN BINS OF DENSITY AND GALACTOCENTRIC RADIUS [a]

Bin	$\mathcal{N}$	$\widehat{\rho}_h$ $[M_\odot\,\mathrm{pc}^{-3}]$	$\widehat{r}_{gc}$ [kpc]	$M_{\min}$ $[M_\odot]$	$M_{\max}$ $[M_\odot]$	$\widehat{M}$ $[M_\odot]$	M_{TO} $[M_\odot]$
ρ_h bins							
$0.034 \leq \rho_h \leq 76.5\ M_\odot\,\mathrm{pc}^{-3}$	48	8.48	12.9	5.63×10^2	8.84×10^5	4.12×10^4	3.98×10^4
$78.8 \leq \rho_h \leq 526\ M_\odot\,\mathrm{pc}^{-3}$	49	232	5.6	8.37×10^3	1.67×10^6	1.22×10^5	1.58×10^5
$579 \leq \rho_h \leq 5.65 \times 10^4\ M_\odot\,\mathrm{pc}^{-3}$	49	973	3.2	1.93×10^4	1.30×10^6	2.82×10^5	2.88×10^5
r_{gc} bins							
$0.6 \leq r_{gc} \leq 3.2$ kpc	47	597	1.9	4.47×10^3	1.02×10^6	1.15×10^5	2.14×10^5
$3.3 \leq r_{gc} \leq 9.4$ kpc	50	261	5.2	2.02×10^3	1.67×10^6	1.27×10^5	1.66×10^5
$9.6 \leq r_{gc} \leq 123$ kpc	49	18.4	18.3	5.63×10^2	1.30×10^6	7.42×10^4	8.71×10^4

[a] The notation $\widehat{x}$ represents the median of quantity x.

where the total mass losses $\Delta_i = (\mu_{ev}\tau)_i$ may differ from cluster to cluster. Given each Δ_i, the normalizations A_i are specified by requiring that the integral over all masses of each term in the summation be unity.

Jordán et al. (2007) refer to a single-component distribution of the form in equation (3) as an evolved Schechter function, and they describe its properties in detail for the case $\beta = 2$. We note only that, at very young cluster ages or for slow mass-loss rates, such that $\Delta_i \ll M_c$, any one evolved Schechter function has a peak at $M_{TO,i} = \Delta_i/(\beta-1)$. As Δ_i increases relative to M_c, the turnover at first increases proportionately, which leads to a decrease in the width of the distribution (since the high-mass end at $M \gtrsim M_{TO,i}$ is largely unchanged). For extreme $\Delta_i \gg M_c$, however, the peak is bounded above by $M_{TO,i} \to M_c$ and the width approaches a lower limit. Any peak in the full equation (3) is a complicated average of the $\mathcal{N}$ individual turnovers and must be calculated numerically.

In their modeling of the Milky Way GCMF, Fall & Zhang (2001) in essence compute distributions of the type (3), with individual Δ_i set by the orbital parameters of clusters in a spherical and static Galactic potential (used both to fix ρ_h, as discussed in §2.1, and to determine additional mass loss due to gravitational shocks). Jordán et al. (2007) fit GCMF data in the Milky Way and scores of Virgo Cluster galaxies with a version of equation (3) in which all GCs have the same Δ_i. They thus estimate the net dynamical mass loss from *typical* clusters in these systems. Here, we construct model GCMFs for the Milky Way using individual Δ_i values given by the observed GC half-mass densities, adopting $\Delta_i \propto \rho_{h,i}^{1/2}$ for evaporation driven by internal relaxation.

We are working from the hypothesis that the mass function of GCs was initially similar to that of young massive clusters, so we fix $\beta = 2$ in equation (3); and we take $M_c = 10^6\ M_\odot$, from the fit to the full Milky Way GCMF by Jordán et al. (2007).[2] Jordán et al. also infer a typical $\widehat{\Delta} = 2.3 \times 10^5 M_\odot$ from their Milky Way fit. Associating this mass loss with the median $\widehat{\rho}_h = 246\ M_\odot\,\mathrm{pc}^{-3}$ of the GCs in Figure 1, we set

$$\Delta = 1.45 \times 10^4\ M_\odot\ \left(\rho_h/M_\odot\,\mathrm{pc}^{-3}\right)^{1/2} \qquad (4)$$

for globulars with any other half-mass density. Assuming an age of 13 Gyr for all GCs in the Galaxy then implies a time-

independent mass-loss rate of

$$\mu_{ev} = 1.1 \times 10^3\ M_\odot\,\mathrm{Gyr}^{-1}\ \left(\rho_h/M_\odot\,\mathrm{pc}^{-3}\right)^{1/2}, \qquad (5)$$

which we discuss in §3.

We now divide the GC sample in Figure 1 roughly into thirds, in two different ways: first on the basis of half-mass density, and second by Galactocentric radius. These ρ_h and r_{gc} bins are defined in Table 1. In each of them we count the clusters in about 10 equal-width bins of $\log M$, to obtain $dN/d\log M$ first as a function of ρ_h and then as a function of r_{gc}. These GCMFs are shown by the points with Poisson errorbars in Figure 2.

As we noted in connection with Figure 1, the typical (either median or turnover) GC mass increases steadily towards higher ρ_h, while the width of the full distribution decreases systematically. Numerical details are given in Table 1. Both features are expected from the behavior of evolved Schechter functions with $\Delta_i \propto \rho_{h,i}^{1/2}$, as described just after equation (3). More physically, and independently of the fine details of the model, when cluster evolution is dominated by evaporation through two-body relaxation, higher-density GCs lose mass more rapidly, implying stronger depletion of a $dN/d\log M_0$ that originally rose monotonically towards low masses.

There are no significant differences between the GCMFs of the two cluster subsamples at $r_{gc} \leq 9.4$ kpc in the right-hand panels of Figure 2, and the main distinction at larger radii is a higher proportion of low-mass clusters. This is just as expected if ρ_h rather than r_{gc} is the parameter of fundamental importance to the GCMF and μ_{ev} increases with ρ_h, since Figure 1 shows that the GC density distribution is insensitive to Galactocentric position for $r_{gc} \lesssim 10$ kpc but has a tail to low $\rho_h \lesssim 10\ M_\odot\,\mathrm{pc}^{-3}$ that is largely confined to $r_{gc} \gtrsim 10$ kpc.

Two model GCMFs are compared to the data in every panel of Figure 2. The dashed curve, which is always the same (apart from normalization), is equation (3) with $\beta = 2$, $M_c = 10^6 M_\odot$, and a fixed $\Delta_i \equiv 2.3 \times 10^5 M_\odot$ (the mass loss from a median-density cluster) for all GCs. This average model, which has a peak at $M_{TO} \simeq 1.6 \times 10^5 M_\odot$, gives a very good description of the observed GCMF in the middle density bin, $79 \lesssim \rho_h \lesssim 530\ M_\odot\,\mathrm{pc}^{-3}$, and of those in the two inner radius bins, $r_{gc} \leq 9.4$ kpc. This is expected, since the median $\widehat{\rho}_h$ in each of these cluster subsamples is very close to the system-wide median of $246\ M_\odot\,\mathrm{pc}^{-3}$, on which the model is based (see Table 1). Even in the outermost r_{gc} bin, a Kolmogorov-Smirnov (KS) test only marginally rejects the

---

[2] Note that M_c appears to take on different values in the GCMFs of other galaxies, varying systematically with the total luminosity L_{gal} (Jordán et al. 2007). The reasons for this are unclear, as is the origin of this mass scale in the first place.
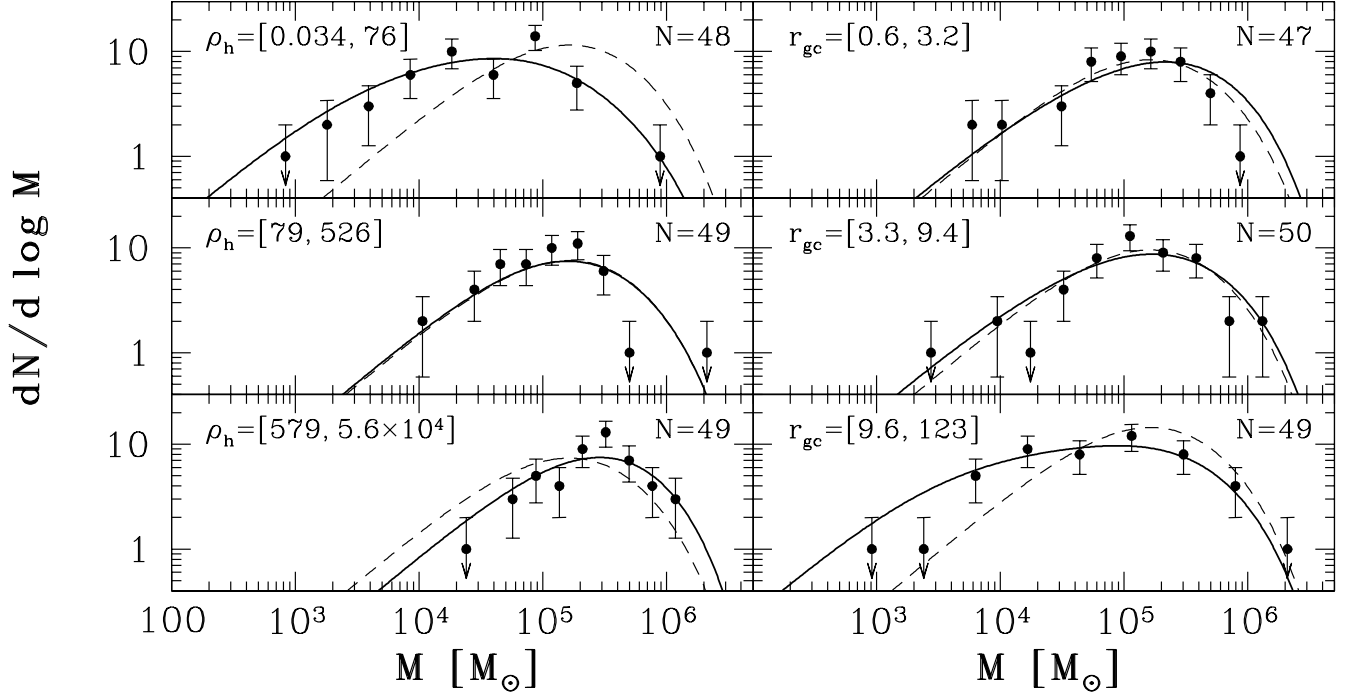
FIG. 2.— GCMF as a function of half-mass density, $\rho_h \equiv 3M/8\pi r_h^3$ (*left panels*), and as a function of Galactocentric radius, r_{gc} (*right panels*), for 146 Milky Way GCs in the catalogue of Harris (1996). The dashed curve in all cases is an evolved Schechter function for the entire GC system (Jordán et al. 2007): equation (3) with $\beta = 2$, $M_c = 10^6\ M_\odot$, and $\Delta_i \equiv 2.3 \times 10^5\ M_\odot$ for all clusters (from eq. [4] and a median $\widehat{\rho}_h = 246\ M_\odot\ \mathrm{pc}^{-3}$), giving a peak at $M_{TO} = 1.6 \times 10^5\ M_\odot$. Solid curves are the GCMFs predicted by equation (3) with $\beta = 2$ and $M_c = 10^6\ M_\odot$ but individual Δ_i given by the observed $\rho_{h,i}$ of each cluster (eq. [4]).

dashed-line model (at the $\simeq 95\%$ level), because this subsample still contains many GCs at or near the global median $\widehat{\rho}_h$ (Figure 1). Again, then, the large scatter in ρ_h versus r_{gc} explains why $dN/d\log M$ is found to depend so weakly on r_{gc}. By contrast, the average GCMF is strongly rejected as a model for the lowest- and highest-density GCs on the left-hand side of Figure 2: the respective KS probabilities that these data are drawn from the dashed distribution are $< 10^{-6}$ and $< 3 \times 10^{-4}$. This is expected as well, since by construction both bins contain only clusters well away from the median density of the full GC system.

The solid curves in Figure 2, which are different in every panel, are the full superpositions of evolved Schechter functions with distinct Δ_i in equation (3) given, through equation (4), by the observed $\rho_{h,i}$ of each cluster in the corresponding subsample. They provide excellent matches to the observed $dN/d\log M$ in every ρ_h and r_{gc} bin; χ^2 per degree of freedom is < 1.3 in all cases. This is the main result of this paper.

Two minor aspects of these solid model curves perhaps bear mentioning. First, they suggest that there may be slightly too few GCs observed with $M \gtrsim 3$–$4 \times 10^5\ M_\odot$ and $\rho_h \lesssim 530\ M_\odot\ \mathrm{pc}^{-3}$ (i.e., in the upper- and middle-left panels of Figure 2). In total, however, only 5 or 6 such clusters are "missing," and the upper-right panel of the figure further shows that any deficit is restricted to small $r_{gc} \lesssim 3$ kpc. If this is an issue at all, it is in a regime of mass and Galactocentric radius for which gravitational shocks and dynamical friction may have been more important than we have allowed. Second, and even less significant, the solid curve in the lower-right panel of Figure 2 appears to predict $\simeq 2$–3 too many clusters with $M \lesssim 5 \times 10^3\ M_\odot$ and $r_{gc} \geq 9.6$ kpc. This most likely reflects the difficulty of detecting very faint and low-surface brightness GCs at very great distances.

The last column of Table 1 gives the peak mass of the (solid) model GCMF for each cluster subsample. These numbers show that $M_{TO} \propto \widehat{\rho}_h^{0.3\text{–}0.4}$, slightly shallower than the $\widehat{\rho}_h^{1/2}$ scaling that might be expected from equations (4) and (5). This is partly because of the averaging of individual turnovers implied by the summation of many evolved Schechter functions, and partly because the individual turnovers themselves grow more slowly than $\Delta_i \propto \rho_{h,i}^{1/2}$ for high Δ_i approaching M_c.

The superposition of many GCMFs with separate, density-dependent turnovers and widths also results in wider $dN/d\log M$ for cluster subsamples covering larger ranges of ρ_h. In particular, this accounts for the shape of the mass function at $r_{gc} \geq 9.4$ kpc. The globulars in this bin span $0.034 \leq \rho_{h,i} \leq 4.1 \times 10^3\ M_\odot\ \mathrm{pc}^{-3}$ (see Figure 1), corresponding to individual evolved Schechter functions with turnover masses $2.7 \times 10^3 \lesssim M_{TO,i} \lesssim 4.0 \times 10^5\ M_\odot$. The composite GCMF in the lower-right panel of Figure 2 thus shows an especially flat and broad peak—so much so that a precise overall M_{TO} cannot be established from the data alone—and a full width at half-maximum much larger than at smaller Galactocentric radii, where the ρ_h distribution is substantially narrower. This explains the findings of Kavelaars & Hanes (1997), who first pointed out that the GCMF of the outermost third of the Milky Way cluster system has a turnover that is statistically consistent with the full-Galaxy average, but a significantly larger dispersion.

Finally, if the GCMF evolved dynamically from initial conditions similar to those we have adopted, then the data in the left-hand panels of Figure 2 taken together disprove the hypothesis that gravitational shocks, rather than relaxation-driven evaporation, might have been the primary cause of it. The (negative) cluster mass-loss rate due to shocks alone is

$\mu_{\rm sh} \propto M/\rho_h \propto r_h^3$, with a constant of proportionality that depends on details of the GC orbit (i.e., the frequency of disk or bulge passages). If the half-mass density were conserved in shock-dominated evolution, as it approximately is when two-body relaxation is dominant, then the GCMFs in different ρ_h bins would differ from each other, and indeed from the initial $dN/d\log M_0$, only in their normalization (Fall & Zhang 2001). This is clearly not the case. If instead it were assumed that r_h is conserved by shocks, then $\mu_{\rm sh}$ would be constant in time and M would have a roughly linear t dependence, as required by the generic M^{+1} scaling of $dN/d\log M$ at low masses. But this would also imply that the GCMF should have a more massive turnover and a narrower width for clusters with larger r_h (faster $\mu_{\rm sh}$), and it is easily confirmed (from the Harris 1996 catalogue again) that the Galactic GCs with the largest half-mass radii are those with the lowest ρ_h. This scenario therefore predicts a GCMF dependence on ρ_h that is exactly opposite to the observations, and to our evaporation-dominated GCMF models with $\mu_{\rm ev} \propto \rho_h^{1/2}$.

2.3. *Other Cluster Properties*

We have not separated the Milky Way GCs into objects with bulge and halo kinematics, nor into metal-rich and metal-poor populations, nor into, say, members of the Sagittarius dwarf spheroidal versus other clusters. Distinct GCMFs can of course be constructed for each of these subsystems or any other, and some are bound to differ from others. But, as with our analysis of the GCMF in radial bins, efforts to understand any differences in $dN/d\log M$ between any other subsamples should focus first and foremost on differences in the clusters' ρ_h distributions.

It is worth exploring one example in detail. Smith & Burkert (2002) note that the mass function of Galactic globulars with King (1966) model concentrations $c < 0.99$ has a somewhat less massive peak than that for $c \geq 0.99$. [Here $c \equiv \log(r_t/r_0)$, where r_t is a fitted tidal radius and r_0 a core scale.] They further show that a power-law fit to the low-c GCMF below its peak returns $dN/d\log M \propto M^{+0.5}$, significantly shallower than the M^{+1} expected generically for a mass-loss rate that is constant in time (and which Smith & Burkert confirm for the GCMF at $c \geq 0.99$). They discuss various options to explain these results, including an ad hoc suggestion that the mass-loss law for low-concentration GCs may have been an explicit function of the instantaneous cluster mass, and thus time-varying. However, they give no physical argument for such a difference, and it is straightforward to see now that none is in fact required.

The upper panel of Figure 3 plots concentration against half-mass density for the same 146 GCs from Figure 1; the filled circles distinguish 24 clusters with $c < 0.99$. There is a correlation of sorts between c and ρ_h, which ultimately either derives from or causes the better-known correlation between c and M (e.g., McLaughlin 2000, and references therein). But more important in the present context is that the ρ_h distribution is offset to lower values and has a higher dispersion at $c < 0.99$. Following the discussion in §2.2, we therefore *expect* the low-concentration GCMF to have a less massive $M_{\rm TO}$, a flatter shape around the peak, and a larger full width than the high-concentration $dN/d\log M$.

The lower panel of Figure 3 shows the GCMFs for $c < 0.99$ (filled circles) and $c \geq 0.99$ (open circles). The curves are again given by equation (3) with $\beta = 2$, $M_c = 10^6\ M_\odot$, and Δ_i related to the observed $\rho_{h,i}$ through equation (4). These
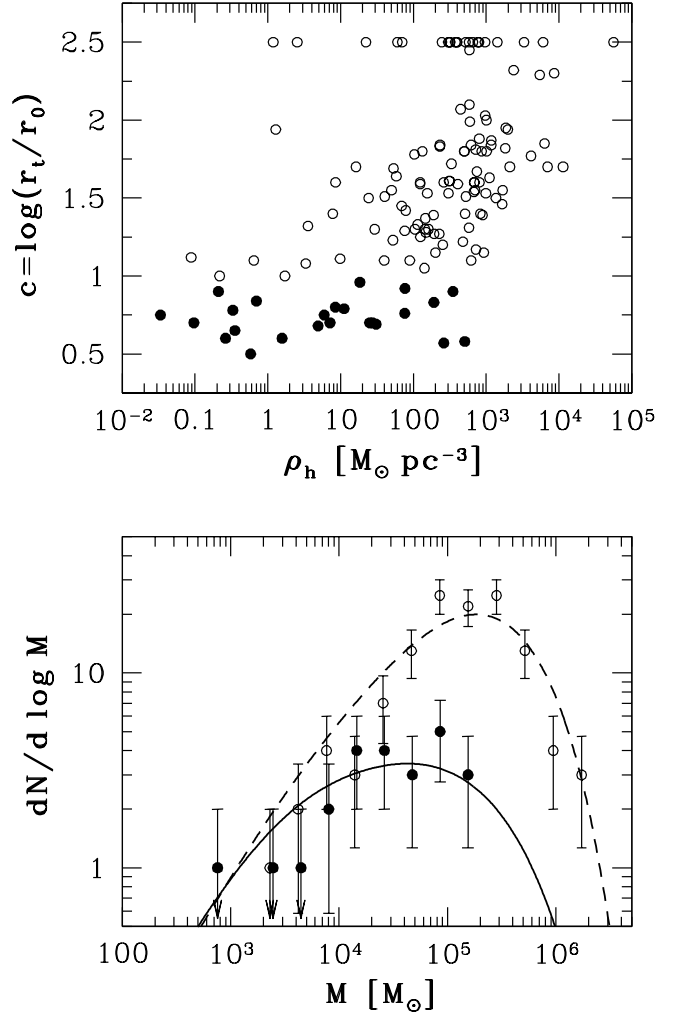

FIG. 3.— *Top:* Concentration parameter as a function of half-mass density for 146 Galactic GCs. The line of points at $c \equiv 2.5$ comes from the practice of *assigning* this value to core-collapsed clusters in the Harris (1996) catalogue and its sources. *Bottom:* GCMF data and models (eqs. [3] and [4]) for 24 clusters with $c < 0.99$ (filled circles and solid curve) and 122 clusters with $c \geq 0.99$ (open circles and dashed curve).

models peak at $M_{\rm TO} \simeq 4.3 \times 10^4\ M_\odot$ for the $c < 0.99$ cluster subsample but at $M_{\rm TO} \simeq 1.8 \times 10^5\ M_\odot$ for $c \geq 0.99$, entirely as a result of the different ρ_h involved. The larger width of $dN/d\log M$ and its shallower slope at any $M \lesssim 10^5\ M_\odot$ for the low-concentration GCs are also clear, in both the data and the model curves. It is further evident that (as Smith & Burkert 2002 also noted) there are no low-c Galactic globulars with $M \gtrsim 2 \times 10^5 M_\odot$, i.e., above the nominal turnover of the full GCMF. But this is not surprising, given that such clusters are so few in number and have such low ρ_h: the solid curve in Figure 3 predicts perhaps $\simeq 3$ high-mass clusters with $c < 0.99$, where none are found.

All aspects of the Milky Way GCMF—including its variations with cluster half-mass density, Galactocentric position, and concentration—are therefore fundamentally consistent with a first-order model for cluster mass loss driven mainly by two-body relaxation, in which $-dM/dt = \mu_{\rm ev} \propto \rho_h^{1/2}$ and ρ_h is constant in time for any given globular. We emphasize again that we have taken the observed distributions of ρ_h versus $r_{\rm gc}$ and of c versus ρ_h simply as given in order to transform $dN/d\log M$ models that depend only on ρ_h, into the curves

matching the data in the right-hand panels of Figure 2 and the bottom of Figure 3. Just as it remains important to understand how the observed $\rho_h(r_{gc})$ distribution came about in a realistic, non-spherical Galaxy evolving in time, so too will an explanation of the empirical $c(\rho_h)$ distribution be of interest.

3. CLUSTER LIFETIMES

The ρ_h-dependent total mass loss per GC in equation (4) corresponds to a μ_{ev} that can obviously be compared to what we might expect from purely theoretical considerations of evaporation. This is most easily done in terms of the total lifetime, $t_{dis} = M_0/\mu_{ev}$, implied for a GC of initial mass M_0. In units of the initial half-mass relaxation time (eq. [8-72] of Binney & Tremaine 1987), equation (5) leads to

$$\frac{t_{dis}}{t_{rh,0}} = \frac{M_0}{\mu_{ev}\,t_{rh,0}} \simeq 0.9\,\ln\Lambda_0 \approx 10\,, \qquad (6)$$

which assumes an average stellar mass of $0.7\,M_\odot$ in all clusters, and where the initial Coulomb logarithm is $\ln\Lambda_0 = 8.7$–13.3 for $M_0 = 10^4$–$10^6\,M_\odot$.

We note that $t_{dis}/t_{rh,0}$ scales with the median GC mass-to-light ratio as $\widehat{\Upsilon}_V^{-1/2}$. This is because Δ and μ_{ev} must scale as $\widehat{\Upsilon}_V$ in order to fit GCMFs derived from cluster luminosities, which are the direct observables. Since $\rho_h^{1/2}$ in equations (4) and (5) already scales as $\Upsilon_V^{1/2}$ (because the luminosity densities are fixed observationally), so too do the numerical coefficients there; but the coefficient in equation (5) then appears in the denominator of equation (6). As described at the beginning of §2.1, we have adopted individual cluster mass-to-light ratios that give $\widehat{\Upsilon}_V \simeq 1.5\,M_\odot L_\odot^{-1}$, which is equal to the median of dynamical estimates for GCs in the Milky Way (McLaughlin 2000; McLaughlin & van der Marel 2005) and in M31 (e.g., Barmby et al. 2007).

As it is, with this very reasonable $\widehat{\Upsilon}_V$, the lifetime in equation (6) appears somewhat short relative to the $t_{dis} \simeq 20$–30 $t_{rh,0}$ normally associated with evaporation due to two-body relaxation alone (e.g., Gnedin & Ostriker 1997). While it is encouraging to find agreement at a factor-of-two level between cluster lifetimes inferred from observations of the GCMF and those found in the theory of two-body relaxation, it is of course important to understand the discrepancy. Each of a few independent factors could go some of the way towards resolving it.

First, we have ignored gravitational shocks to this point. Fokker-Planck calculations that include both relaxation and shocks (with or without a spectrum of stellar masses) show a linear time dependence of the cluster mass, $M(t) \simeq M_0 - \mu_{ev}t$, which is the same behavior we have assumed here (Gnedin, Lee, & Ostriker 1999). In the case of strong shocks, Gnedin, Lee, & Ostriker show that μ_{ev} can be increased, and $t_{dis}/t_{rh,0}$ decreased, by factors between 1 and 2. It is not entirely clear what the average factor is for the whole system of GCs in the Milky Way.

Calculations by Fall & Zhang (2001) and Prieto & Gnedin (2006) indicate that shocks are subdominant compared to two-body relaxation alone and thus that they speed up evaporation by a factor likely closer to 1 than to 2. Moreover, we showed in §2 that the GCMF can be understood in quite some detail if μ_{ev} and t_{dis} are essentially the same for all GCs of a given half-mass density wherever they are in the Galaxy. If repeated strong shocks are invoked to increase μ_{ev} by a *typical* factor of 2 over its relaxation-only values, it is not easy to see how this

could be achieved equally for clusters near the Galactic center and in the outer halo, where we might expect shocks to be weaker and less frequent. On the other hand, we have argued that the complexity of the observed GC $\rho_h(r_{gc})$ distribution is essentially the result of clusters having formed in many progenitor galaxies, which were eventually incorporated into the present-day Milky Way through a series of mergers and accretions. It may be that the gravitational shocking of globulars while in their progenitors, or even during their accretion into the Galaxy, could similarly help explain a uniformly enhanced μ_{ev} that still scales primarily as $\rho_h^{1/2}$ without a significant dependence on the current r_{gc}.

Second, there are uncertainties in the theoretical t_{dis} for two-body relaxation even without gravitational shocks. Different numerical methods give results differing at the $\sim 30\%$–40% level, depending on the detailed form of the stellar distribution function at near-escape energies and on the precise criteria adopted to decide when an individual star has escaped a cluster; see, e.g., Giersz (2001) and references therein. Also along these lines, it is worth mentioning that the rule of thumb $t_{dis} \simeq 20$–30 $t_{rh,0}$ generally holds for clusters of stars with a single mass. However, relaxation in GCs with realistic stellar mass functions can lead to complete evaporation on shorter timescales (e.g., Johnstone 1993; Lee & Goodman 1995; Giersz 2001).

And third, our numerical values for Δ and μ_{ev} as functions of ρ_h are specific to the value $\beta = 2$ for the power-law exponent of the initial GCMF at low masses (eq. [2]). As we noted just after equation (3), the turnover mass of an evolved Schechter function is $M_{TO} \simeq \Delta/(\beta-1)$ in the limit of very low half-mass density, and $M_{TO} \to M_c$ for high ρ_h. In this sense, Δ is most strongly constrained by the low-density clusters. All other things being equal, their observed GCMF can be reproduced with $\beta \neq 2$ if Δ and μ_{ev} are multiplied by $(\beta-1)$ at fixed ρ_h in equations (4) and (5). Equation (6) then becomes $t_{dis}/t_{rh,0} \approx 10/(\beta-1)$. Observations of young massive clusters (e.g., Zhang & Fall 1999) constrain β to be rather near 2; but if it were slightly shallower, then our inferred t_{dis} would increase accordingly (by 25% if $\beta = 1.8$, for example).

4. CONCLUSIONS

We have emphasized that models for dynamical evolution of the GCMF, in which an initial power-law mass distribution rising steeply below the present-day peak M_{TO} is depleted predominantly by cluster evaporation driven by two-body relaxation, inevitably predict that $dN/d\log M$ should depend on cluster half-mass density, ρ_h. We have shown that the Galactic GCMF exhibits just the dependence expected, with M_{TO} increasing and the width of the distribution decreasing as ρ_h increases. The observations are quantitatively well matched by a mass-loss rate, $\mu_{ev} \propto \rho_h^{1/2}$ with ρ_h constant in time, adopted here as a first-order description of relaxation-driven evaporation. The same data therefore rule out GCMF evolution driven primarily by gravitational shocks (since mass loss from shocks is greater at lower cluster densities, opposite to evaporation).

We have also shown that the weak dependence of the GCMF on Galactocentric radius, r_{gc}, follows from its strong dependence on cluster ρ_h, given the complex $\rho_h(r_{gc})$ distribution actually observed. Although we have not attempted to explain this $\rho_h(r_{gc})$ relation—doing so will require sophisticated modeling of GC system evolution in a non-spherical and time-dependent Galaxy growing in a hierarchical cosmology—our

results negate arguments against evaporation-driven evolution of the GCMF based on weak or absent radial gradients in the turnover mass M_{TO} (cf. Vesperini et al. 2003).

Similarly, the observation that Galactic globulars with low concentrations c have a significantly different $dN/d \log M$ from high-concentration clusters is a natural consequence of the basic density dependence of the GCMF and the fact that low- and high-c GCs have quite different ρ_h distributions. There is no need to invoke different mass-loss laws for the two types of cluster.

The normalization of the mass-loss rate $\mu_{ev} \propto \rho_h^{1/2}$ that fits the Galactic GCMF data implies cluster lifetimes $t_{dis} \approx 10\, t_{rh,0}$—about a factor of two shorter than usual in standard theories for the relaxation-driven evaporation of clusters of single-mass stars. Understanding this discrepancy may depend in part on a closer examination of enhanced stellar escape rates from the outer regions of clusters affected by gravitational shocks (even if shocks are not the main catalysts of the overall cluster evolution). Another possibility is the faster escape of stars from clusters with a realistic distribution of stellar masses.

REFERENCES

Aarseth, S. J., & Heggie, D. C. 1998, MNRAS, 297, 794
Barmby, P., Huchra, J. P., & Brodie, J. P. 2001, AJ, 121, 1482
Barmby, P., McLaughlin, D. E., Harris, W. E., Harris, G. L. H., & Forbes, D. A. 2007, AJ, in press
Baumgardt, H. 1998, A&A, 330, 480
Baumgardt, H., & Makino, J. 2003, MNRAS, 340, 227
Binney, J., & Tremaine, S. 1987, Galactic Dynamics (Princeton: Princeton University Press)
Burkert, A., & Smith, G. H. 2000, ApJ, 542, L95
Elmegreen, B. G., & Efremov, Y. N. 1997, ApJ, 480, 235
Fall, S. M., & Rees, M. J. 1977, MNRAS, 181, 37P
Fall, S. M., & Zhang, Q. 2001, ApJ, 561, 751
Giersz, M. 2001, MNRAS, 324, 218
Gnedin, O. Y., & Ostriker, J. P. 1997, ApJ, 474, 223
Gnedin, O. Y., Lee, H. M., & Ostriker, J. P. 1999, ApJ, 522, 935
Harris, W. E. 1996, AJ, 112, 1487
Harris, W. E. 2001, in Star Clusters (28th Saas-Fee Advanced Course) ed. L. Labhardt & B. Binggeli (Berlin: Springer), 223
Harris, W. E., & Pudritz, R. E. 1994, ApJ, 429, 177
Harris, W. E., Harris, G. L. H., & McLaughlin, D. E. 1998, AJ, 115, 1801
Johnstone, D. 1993, AJ, 105, 155
Jordán, A., et al. 2005, ApJ, 634, 1002
Jordán, A., et al. 2006, ApJ, 651, L25
Jordán, A., et al. 2007, ApJS, in press (astro-ph/0702496)
Kavelaars, J. J., & Hanes, D. A. 1997, MNRAS, 285, L31
Lee, H. M., & Goodman, J. 1995, ApJ, 443, 109
King, I. R. 1966, AJ, 71, 276
McLaughlin, D. E. 1994, PASP, 106, 47
McLaughlin, D. E. 2000, ApJ, 539, 618
McLaughlin, D. E., & van der Marel, R. P. 2005, ApJS, 161, 304
Murali, C., & Weinberg, M. D. 1997, MNRAS, 291, 717
Prieto, J. L., & Gnedin, O. Y. 2006, preprint (astro-ph/0608069)
Schechter, P. 1976, ApJ, 203, 297
Smith, G. H., & Burkert, A. 2002, ApJ, 578, L51
Spitzer, L. 1987, Dynamical Evolution of Globular Clusters (Princeton: Princeton Univ. Press)
Vesperini, E. 1998, MNRAS, 299, 1019
Vesperini, E., & Heggie, D. C. 1997, MNRAS, 289, 898
Vesperini, E., & Zepf, S. E. 2003, ApJ, 587, L97
Vesperini, E., Zepf, S. E., Kundu, A., & Ashman, K. M. 2003, ApJ, 593, 760
Zhang, Q., & Fall, S. M. 1999, ApJ, 527, L81